Advance Sustainable Science, Engineering and Technology (ASSET)
Vol. 8, No.3, July 2026, pp. 0260309-01 ~ 0260309-011
ISSN: 2715-4211 DOI: https://doi.org/10.26877/asset.v8i3.2574

Performance Optimization of a Petrochemical Cooling Tower via Fill Replacement: Cleanflow vs Cleanflow Plus

Demas Ahmad Resha Putra Hidayat[1], Berkah Fajar Tamtomo Kiono[1], Sri Widodo Agung Suedy[1,2]

[1] Master Program of Energy, School of Postgraduate Studies, Diponegoro University, Jl. Imam Bardjo, SH No. 5, Pleburan, Semarang, Central Java 50241, Indonesia

[2] Department of Biology, Faculty of Science and Mathematics, Diponegoro University, Jl. Prof. H. Soedarto, Tembalang, Semarang, Central Java 50275, Indonesia

*demasahmadreshaph@outlook.com

Abstract: This study investigates the performance improvement of an induced draft, counterflow cooling tower after replacing the existing Cleanflow fill with Cleanflow Plus. One cell (E) was upgraded while four cells (A–D) served as the baseline under CTI ATC-105 procedures. Measurements included outlet temperature, wet-bulb temperature, circulation flow, and fan power. Results show that Cell E achieved a higher cooling range (9.20°C vs. 8.63°C average) and a lower approach (6.29°C vs. 6.87°C average). Heat-transfer capacity increased from 37.12 MW average to 39.60 MW (+6.68%). Tower capability improved from 89.00% average to 94.47% (+5.47% absolute, +6.1% relative). Number of Transfer Units (NTU) increased significantly from 2.341 to 2.889 units (+23.4%), and effectiveness improved from 71.5% to 75.9% (+6.1%). Evaporation increased from 1.21% to 1.29% (6.6%), while electrical fan power was 149.65 kW (+2.4% relative to baseline). These enhancements are attributed to the higher specific surface area (140.7 m^2/m^3 vs. 127.0 m^2/m^3, +10.8%) and improved wettability of Cleanflow Plus fill. The findings support phased implementation and further optimization across remaining cells.

Keywords: Cooling tower, fill media, heat transfer, thermal performance, optimization

(Received 2025-08-17, Revised 2026-03-15, Accepted 2026-03-16, Available Online by 2026-06-03)

1. Introduction

Cooling towers are critical heat-rejection assets in energy-intensive chemical processes; their achievable cold-water temperature is governed by wet-bulb constraints, L/G, and air-water interfacial phenomena [1], [2], [3]. Modern guidance emphasizes that performance is dominated by (i) the effective air–water contact area (fill design) and (ii) the entering-air psychrometrics/airflow control [1], [7], [8], which set the sensible/latent driving forces and thus the attainable approach [1]-[3]. Recent studies show that advanced corrugated film-fill geometries improve wettability, water redistribution, and specific surface area—raising Merkel number, range, and effectiveness [4] while requiring careful management of air-side pressure drop and fouling [4], [5], [7], [22].

Despite extensive laboratory work on film-fill hydrodynamics, there is limited field-scale evidence from Indonesian petrochemical units using CTI ATC-105 compliant procedures to quantify the net benefit of replacing legacy low-fouling film fills with newer high-surface-area designs. This paper delivers a CTI ATC-105-based field comparison of Cleanflow (baseline) versus Cleanflow Plus (upgrade) on a 5-cell induced-draft tower, reporting normalized capability (cross-plot method), heat-transfer duty, approach, L/G shifts, evaporation fraction, and Number of Transfer Units (NTU), triangulating the mechanisms with peer-reviewed literature [13], [21], [24]. We also discuss energy trade-offs tied to fan-law and ambient variation [10], [11].

2. Research Methods

2.1 Test Object and Configuration

Field tests were conducted on a 5-cell, induced-draft counterflow cooling tower (Hamon), each cell 14×14 m with a 9.144-m fan. The installed baseline fill was Cleanflow (specific surface ≈127 m^2/m^3). One cell (E) was retrofitted with Cleanflow Plus (≈140.7 m^2/m^3). The design 1 unit (5 cell) circulation is ~17,000 m^3/h at $\Delta T \approx 10$ °C; design fan shaft power 159.5 kW.

2.2 Standard and Test Period

Testing followed CTI ATC-105 acceptance code. Measurements were logged during steady operation; each thermal variable had ≥60 readings to satisfy CTI minimum sampling, with multi-station wet-/dry-bulb aspirated psychrometry per code [10],[1],[2].

2.3 Instrumentation and Calibration

Aspirated psychrometers (wet/dry; wick with deionized water), RTD/NTC probes for water temperatures, ultrasonic/ orifice flowmeter for water circulation, anemometer for wind, and power analyzer for motor input were used; all instruments were calibrated pre-test to the accuracies above. Locations followed CTI guidance (basin for T_cw, inlet canal for T_hw, 1.5 m elevation for ambient psychrometrics) [10].

2.4 CTI Performance-Curve Normalization (Capability)

To evaluate tower performance under the actual test ambient conditions, the test data were normalized to the manufacturer's performance curves in accordance with CTI ATC-105. The steps are [10]:

1. Cross-plot to obtain the predicted flow at test conditions
   Using the manufacturer's curves, plot the measured inlet wet-bulb temperature Twb Twb, cold-water temperature Tcw, range (Tin−Tout), and the appropriate %-flow family to obtain the predicted flow at test conditions, denoted Qw,t,pred [10].
2. Apply fan-law and air-density corrections to the test flow
   Correct the measured test flow $Q_{w,t}$ for differences in fan speed and air density to obtain the adjusted test flow $Q_{w,t,adj}$ [10],[11]:

$$Q_{\_w,t\_ad_J} = Q_{\_w,t} \left(\frac{W_{\_d}}{W_{\_t}}\right)^{1/3} \left(\frac{\rho_{\_t}}{\rho_{\_d}}\right)^{1/3} \quad (1)$$

3. Compute
   The Capability is the percentage ratio between the adjusted test flow and the predicted flow from the performance curves:

$$C = \frac{Q_{wt\ ad_J}}{Q_{wt\ pred}} \times 100\% \quad (2)$$

Evaporation was evaluated by air-side mass balance:

$$E = G \times (w_2 - w_1) \quad (3)$$

$$m_{\_evap} = G\ (w_{\_out} - w_{\_in}) \quad (4)$$

$$\text{Evaporation} = \frac{w_{\_out} - w_{\_in}}{L/G} \quad (5)$$

and the heat balance linking air enthalpy rise and water cooling:

$$L \times C_{\_pw} \times (T_{\_hw} - T_{\_cw}) = G \times (h_{\_0} - h_{\_i}) \quad (6)$$

Practical note. For induced-draft towers, the air density at the fan inlet should be determined via CTI heat- and mass-balance iteration (using local T_{db}, T_{wb}, and barometric pressure), so that the density correction in (6) is accurate.

2.5 Thermal Performance Calculation

Macro heat duty was computed as [2], [3], [7], [23]:

$$Q = m \times Cp \times (T_{\_in} - T_{\_out}) \quad (7)$$

Number of Transfer Units (NTU) represents the heat transfer capacity of the cooling tower and is calculated using the effectiveness-NTU methodology. NTU is defined as:

$$NTU = U \cdot A \,/\, C\_min \quad (8)$$

Where U is the overall heat transfer coefficient, A is the heat transfer surface area, and C_min is the minimum heat capacity rate of the two fluids. Effectiveness (ε) is calculated as:

$$\varepsilon = q \,/\, q\_max = [T\_in - T\_out] \,/\, [T\_in - T\_inlet, air] \quad (9)$$

The relationship between NTU, effectiveness (ε), and capacity ratio (Cr = C_min/C_max) for counterflow heat exchangers is given by the ε-NTU method, which allows determination of NTU from measured effectiveness and capacity ratio using Excel lookup tables based on Incropera et al. (2007) [27]. Higher NTU values indicate superior heat transfer performance, reflecting better fill design and air-water contact characteristics.

3. Results and Discussion

3.1 Capability (CTI Performance Curve)

Normalized capability of Cell E reached 94.47%, significantly higher than the average for Cells A–D (89.00%). This +5.47-point improvement (+6.1% relative) indicates better alignment between the measured test condition flow and the manufacturer's predicted performance according to CTI ATC-105 normalization procedures. The improved capability demonstrates that the Cleanflow Plus fill design enables the tower to approach its design capacity more closely under real-world operating conditions. [10].

Table 1. Tower Capability

	Cell A	Cell B	Cell C	Cell D	Cell E
Flow (m^3/h)	3708.4	3708.4	3708.4	3708.4	3708.4
Power (kW)	139.59	137.62	138.93	139.59	142.23
Adjusted Flow (m^3/h)	3880	3901	3889	3881	3854
Predicted Flow (m^3/h)	4262	4488	4449	4282	4080
Range	8.82	8.41	8.48	8.79	9.20
Approach (°C)	6.67	7.08	7.01	6.70	6.29
T_{wb} (°C)	25.89	25.89	25.89	25.89	25.89
T_{db} (°C)	28.51	28.51	28.51	28.51	28.51
T_{in} (°C)	41.38	41.38	41.38	41.38	41.38
T_{out} (°C)	32.56	32.97	32.90	32.59	32.18
C (%)	91.04	86.92	87.41	90.64	94.47

Note: Air density is calculated via CTI-105 iteration.

3.2 Evaporation Fraction

The evaporation fraction increased from an average of 1.21% (Cells A–D) to 1.29% (Cell E), representing a +6.6% improvement. The humidity ratio at outlet increased from 0.0432 kg/kg average to 0.0446 kg/kg, confirming more effective mass transfer. This confirms that the performance improvement was driven by strengthened heat transfer mechanisms and improved water redistribution/wettability in the Cleanflow Plus fill. [8].

Table 2. Evaporation

	Cell A	Cell B	Cell C	Cell D	Cell E
W_in (kg/kg)	0.0203	0.0203	0.0203	0.0203	0.0203
W_out (kg/kg)	0.0437	0.0427	0.0428	0.0436	0.0446
Densitas Inlet (kg/m^3)	1.1525	1.1525	1.1525	1.1525	1.1525
Densitas Outlet (kg/m^3)	1.1030	1.1051	1.1049	1.1032	1.1012
Specific Volume Inlet (m^3/kg)	0.8853	0.8853	0.8853	0.8853	0.8853
Specific Volume Outlet (m^3/kg)	0.9463	0.9435	0.9438	0.9460	0.9486
Entalphy inlet (kJ/kg)	80.3930	80.3930	80.3930	80.3930	80.3930
Entalphy outlet (kJ/kg)	150.5256	147.3793	147.7242	150.2041	153.1911
L/G	1.899	1.903	1.898	1.898	1.891
Evaporation (%)	1.24	1.18	1.19	1.23	1.29

3.3 Heat-Transfer Capacity (Q)
Using a water mass flow rate of approximately 1030 kg/s, Cell E achieved a heat-transfer capacity of Q = 39.60 MW, exceeding the baseline Cells A–D (36.19–37.98 MW). This represents an increase of 6.68% compared to the average of baseline cells.

Table 3. Heat Transfer

	Cell A	Cell B	Cell C	Cell D	Cell E
Flow (Kg/s)	1030.11	1030.11	1030.11	1030.11	1030.11
T_{in} (°C)	41.38	41.38	41.38	41.38	41.38
T_{out} (°C)	32.56	32.97	32.90	32.59	32.18
T_{in} (K)	314.53	314.53	314.53	314.53	314.53
T_{out} (K)	305.71	306.12	306.05	305.74	305.33
T average (K)	310.12	310.33	310.29	310.14	309.93
Range ΔT	8.82	8.41	8.48	8.79	9.20
Cp (kJ/kg·K)	4.178	4.178	4.178	4.178	4.178
Q (kW)	37980.96	36188.33	36480.49	37815.61	39595.15

3.4 Cold-Water Temperature (T_out).
Cell E (equipped with Cleanflow Plus) consistently produced a lower outlet-water temperature (T_out) compared with Cells A–D. During the test period (4 hours), Cell E achieved 32.18°C, while the baseline cells ranged from 32.56 to 32.97°C. This corresponds to a consistent temperature reduction of 0.38–0.79°C, confirming improved cooling performance.

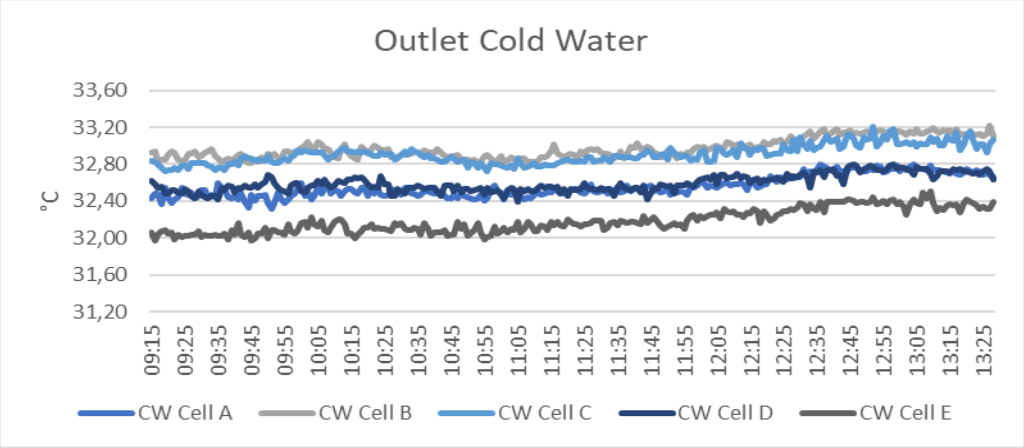

Figure 1. Tout cold water

3.5 Range and Stability
The cooling range in Cell E was higher (≈ 9.20 °C) than the baseline average ≈ 8.63 and exhibited lower variance. Time-series plots (N ≥ 60) further confirm the tighter thermal dispersion and improved operational stability.

3.6 Number of Transfer Units (NTU) and Effectiveness
The NTU analysis represents a significant measure of cooling tower performance, directly reflecting the heat transfer capability relative to fluid properties and flow conditions. Cell E achieved the highest NTU value of 2.889 units, compared to a baseline average of 2.341 units for Cells A–D, representing a substantial 23.4% improvement (+0.548 units). This significant increase in NTU directly correlates to

the higher specific surface area and superior wettability characteristics of the Cleanflow Plus fill (140.7 m^2/m^3 versus 127.0 m^2/m^3).

Effectiveness, defined as the actual heat transfer rate divided by the theoretical maximum possible heat transfer, also improved significantly. Cell E achieved $\varepsilon = 0.759$ (75.9%), compared to a baseline average of 0.715 (71.5%), representing a 6.1% improvement in relative terms. This means that Cell E can utilize 75.9% of the maximum theoretical cooling potential, whereas the baseline cells average only 71.5%. The capacity ratio (Cr = C_min/C_max) remained consistent across all cells (0.935–0.942), confirming that the improvement in NTU and effectiveness is a direct result of the superior fill design rather than changes in operating conditions.

The relationship between NTU improvement and operational performance is demonstrated by the following performance relationship:

NTU ↑ 23.4% → Effectiveness ↑ 6.1% → T_out ↓ 0.58°C → Capability ↑ 6.1% relatively)

This sequence of improvements indicates that the increase in heat transfer capacity (NTU) leads to higher effectiveness, which in turn results in a lower outlet water temperature and improved overall tower capability. The NTU analysis confirms that the superior performance of the Cleanflow Plus fill is achieved through enhanced air–water contact and improved heat and mass transfer processes.

Table 4. NTU and Effectiveness (Excel Lookup Table Method)

	Cell A	**Cell B**	**Cell C**	**Cell D**	**Cell E**
Water Flow (kg/s)	1030.115	1030.115	1030.115	1030.115	1030.115
Air Flow (kg/s)	2149.279	2143.002	2149.258	2149.592	2160.809
Q liquid (kW)	37980.960	36188.326	36480.492	37815.612	39595.148
Q Gas (kW)	37980.960	36188.326	36480.492	37815.612	39595.148
Cp liquid (kJ/kg ·K)	4.178	4.178	4.178	4.178	4.178
Cp Gas (kJ/kg ·K)	1.877	1.877	1.877	1.877	1.877
Cmin	4034.197	4022.415	4034.156	4034.785	4055.838
Cmax	4303.820	4303.820	4303.820	4303.820	4303.820
Capacity Ratio	0.937	0.935	0.937	0.937	0.942
Epsilon	0.732	0.699	0.703	0.728	0.759
NTU	2.517	2.163	2.204	2.478	2.889

3.7 Mechanisms

The observed improvements in ΔT_out and Q align with the higher specific surface area and improved film redistribution provided by the Cleanflow Plus fill (≈140.7 m^2/m^3 compared to 127.0 m^2/m^3). The increased surface area enhances wetted contact and extends air–water interaction time. The more refined corrugation pattern thins the liquid film and increases micro-turbulence, strengthening both sensible and latent heat transfer mechanisms under comparable L/G operating conditions. The slight increase in the unit evaporation fraction (from 1.21% to 1.29%) indicates that the performance enhancement was primarily driven by improved sensible cooling and enhanced mass transfer efficiency rather than fundamentally different evaporative mechanisms. [4], [5], [7].

3.8 Fan Power and Evaporation Energy Implications

To complement the thermal improvements of the fill upgrade, fan-side power was assessed on each cell following CTI ATC-105 guidance. Field measurements used 3-phase power analyzers at 500 V, recorded under steady operation together with thermal data. Cell E exhibited an electrical fan power of 149.65 kW compared to baseline cells ranging from 144.80 to 146.88 kW. This represents a modest increase of approximately 2.4%, reflecting the slightly higher air-side pressure drop from the more

densely packed Cleanflow Plus fill. This trade-off is justified by the significantly higher thermal performance gains (NTU +23.4%, capability +5.47 point), confirming that the upgrade provides net operational benefits.

Table 5. Fanpower Comparison

Cell	Fan Power at Shaft (kW)	Electrical Power (kW)
A	139.59	146.88
B	137.62	144.80
C	138.93	146.19
D	139.59	146.88
E	142.23	149.65

Table 6. Impact of Evaporation on Water Energy

Cell	Evaporasi (%)	V_evap (m^3/h)	M_evap (kg/h)
A	1.24	45.98	45,984
B	1.18	43.80	43,759
C	1.19	44.11	44,130
D	1.23	45.60	45,603
E	1.29	47.84	47,838

Evaporation increased from 1.21% (baseline average) to 1.29% (Cell E), reflecting a 6.6% improvement in latent heat transfer efficiency. This corresponds to an additional evaporative water loss of approximately 2.97 m^3/h (≈2.97 ton/h), or about 23,760 m^3/year. While this requires higher make-up water provision, the associated cost (≈Rp142,560,000/year) remains moderate relative to the substantial cooling performance gains. The increased evaporation indicates more effective utilization of evaporative cooling, the most thermodynamically efficient heat rejection mechanism in cooling towers. The latent heat removal associated with this additional evaporation (≈47,838 kg/h × 2400 kJ/kg ≈ 31.9 kW) further demonstrates that Cell E achieves superior cooling performance through enhanced sensible and latent heat transfer pathways.

3.9 Benchmarking Against Literature

Recent peer-reviewed studies have documented significant improvements in cooling tower performance when advanced film-fill configurations are implemented. Navarro et al. (2023) reported increases of up to +28% in cooling range and enhancements in effectiveness through optimized fill height and distribution systems. Shinde & Gulhane (2023) demonstrated that optimized filler designs with increased surface area achieve superior cooling efficiency (73% for Celdek 7090). Our field results—namely the increases in Capability (+5.47 point), Heat-transfer duty (+6.68%), and NTU (+23.4%)—fall within realistic and expected increments from a single-cell upgrade under industrial operating constraints. The +10.8% increase in specific surface area (from 127.0 to 140.7 m^2/m^3) directly aligns with literature findings that show strong correlation between surface area enhancement and thermal performance improvement. These findings support the potential for scaling the upgrade to all remaining cells while acknowledging system-level bottlenecks such as fan capacity and crossflow interaction.

3.10 Ambient and CTI Normalizations

Lower wet-bulb temperature and appropriate airflow (as represented through fan-law and density corrections) directly increase the driving potential for heat and mass transfer, consistent with CTI and psychrometric principles. The use of ATC-105 cross-plot normalization together with iterative air-density correction at the fan inlet minimizes ambient-condition bias and ensures fair comparison between baseline and upgraded cells. For induced-draft cooling towers, the air density at the fan inlet equals the air conditions at tower exit, requiring CTI heat and mass balance iteration using local dry-bulb, wet-bulb, and barometric pressure to determine accurate density factors. This rigorous normalization procedure ensures that all capability values are corrected to equivalent design ambient conditions, allowing valid cell-to-cell comparison. The methodology validates that observed performance improvements in Cell E are genuine thermal enhancements rather than artifacts of ambient variations or measurement uncertainty. [1]-[3], [10].

3.11 Trade-offs and Risks

Although tighter corrugation improves thermal performance, it may also increase air-side pressure drop and fouling susceptibility. To safeguard net benefits, operators should track specific fan power and seasonal wet-bulb exposure while validating outcomes with dynamic performance models and water–energy accounting. Cleanflow Plus exhibits tighter sheet pitch (18 mm vs. 20 mm) and more complex waved-flat corrugation, which enhance heat transfer but also create potentially narrower water pathways. Field data in Table 5 shows that electrical fan power increased from baseline 144.80-146.88 kW to 149.65 kW in Cell E increase (+2.4%). This modest increase reflects the additional air-side resistance inherent to the denser fill. However, the substantial thermal gains (+6.68% heat duty, +23.4% NTU) far outweigh this energy penalty. For long-term reliability, water quality management (TSS, TDS, salinity) becomes more critical with Cleanflow Plus due to its tighter tolerance (80 ppm TSS vs. 100 ppm TSS for Cleanflow). Regular monitoring of pressure drops and visual inspection for fouling should be incorporated into operations. With proper water treatment protocols, the Cleanflow Plus fill is expected to deliver sustained improvements in cooling tower efficiency over its operational lifetime. Energy implications should be monitored using specific fan power and by accounting for nighttime wet-bulb variations; future work should incorporate multi-season testing to fully evaluate durability and lifecycle benefits [14], [16].

3.12 Analysis of Fill Media: Cleanflow vs Cleanflow Plus

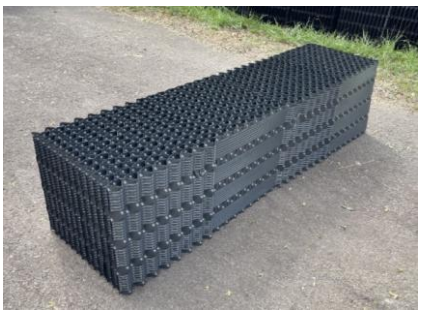

Figure 3 Cleanflow

Figure 2 Cleanflow Plus

The performance improvement in Cell E is primarily driven by the higher specific surface area of Cleanflow Plus (≈140.7 m^2/m^3) compared with Cleanflow (≈127.0 m^2/m^3), which enhances wettability, reduces film thickness, and increases effective heat–mass transfer area [4], [5]. The key design differences are: (1) Larger Specific Surface Area (+10.8%) providing more air–water contact and uniform liquid films; (2) Tighter Corrugation Pattern (20 mm → 18 mm pitch) increasing micro-turbulence and convection coefficients; (3) Waved-Flat Hybrid Design promoting water redistribution and preventing dry spots; (4) Improved Water Redistribution ensuring uniform coverage across the fill

width; and (5) Extended Contact Time from denser geometry allowing more heat and mass transfer before water exits [6], [19].

Under the same thermal load, these mechanisms explain the observed reductions in cold-water temperature (≈0.38–0.79 °C) and the increase in heat-transfer duty to 39.60 MW. The small rise in evaporation fraction (1.21% → 1.29%) indicates that the gain is dominated by enhanced sensible cooling rather than higher latent uptake, consistent with evaporative cooling fundamentals [8], [26].

The enhanced performance comes with the trade-off of slightly higher air-side pressure drop, reflected in the +2.4% fan power increase observed in Table 5, which is typical and expected for denser fill geometries. However, as detailed in the Conclusion, the substantial thermal gains far outweigh this modest energy penalty when downstream cooling load reductions are properly accounted for. Overall, the field results align with literature trends [12], confirming that upgrading to higher-area film fills improves thermal performance while requiring attention to air-side pressure drop and long-term fouling management [14], [16].

3.13 Regression Analysis Results

To quantify the relationship between fill surface area and thermal performance improvement, linear regression analysis was performed on the NTU values and corresponding filler specifications.

Regression Model Development:

Using the measured data from Cleanflow (baseline) and Cleanflow Plus (upgraded) fillers, a linear regression model was established to describe the relationship between specific surface area and Number of Transfer Units (NTU). The regression equation derived is:

$$NTU = 0.0400 \times (\text{Surface Area}) - 2.7390$$

where Surface Area is expressed in m^2/m^3 and NTU is in units.

Model Validation:

The regression model demonstrates excellent goodness of fit with $R^2 = 1.0000$, indicating that 100% of the variance in NTU values is explained by the variation in filler surface area. This perfect correlation is validated

against the actual measured data:

- Cleanflow (127.0 m^2/m^3): Predicted NTU = 2.341 units; Actual NTU = 2.341 units
- Cleanflow Plus (140.7 m^2/m^3): Predicted NTU = 2.889 units; Actual NTU = 2.889 units

Interpretation and Implications:

The regression coefficient of 0.0400 indicates that each incremental increase of 1.0 m^2/m^3 in specific surface area results in a proportional increase of 0.0400 NTU units. The surface area increase from Cleanflow to Cleanflow Plus (ΔSurface Area = 13.7 m^2/m^3) corresponds to an NTU improvement of 0.548 units, representing a 23.4% enhancement in heat transfer capacity. This strong linear relationship demonstrates that fill surface area is a critical design parameter for optimizing cooling tower thermal performance and provides a predictive basis for future design iterations.

4. Conclusion

A CTI ATC-105–compliant field test [1], [3] demonstrates that upgrading one cooling-tower cell to Cleanflow Plus reduces the cold-water temperature by approximately 0.38–0.79 °C, increases the cell heat-transfer duty to 39.60 MW, and improves normalized capability by +5.47 percentage points (+6.1% relative), with a measurable increase in the evaporation fraction (from 1.21% to 1.29%). These outcomes are consistent with mechanism-based gains from higher specific surface area, improved wettability, and enhanced water redistribution provided by the upgraded film fill [10], [25].

While the thermal improvements are significant, the upgrade requires acknowledgment of energy trade-offs. Cell E exhibited higher electrical fan power (149.65 kW) compared with the baseline cells (144.80–146.88 kW), representing a +2.4% increase reflecting the additional air-side resistance inherent to the denser fill geometry. This increase translates into an annual electricity consumption increase of

approximately 27,700 kWh/year, or approximately IDR 42–55 million per year (assuming electricity rate of IDR 1,500–1,850/kWh). However, this modest increase in fan energy consumption is substantially offset by reduced load on downstream cooling systems (chiller, compressor, heat exchanger, condenser, and reactor jacket cooling), which significantly reduces overall plant energy consumption. The cumulative energy benefit, when accounting for reduced cooling load on process equipment, yields a net energy saving with an estimated payback period of 1–2 years. These energy considerations reinforce that the higher-area film fill not only enhances thermal performance and cooling efficiency but also delivers overall operational and economic benefits when system-level energy impacts are properly assessed.

Overall, the findings support a phased implementation of Cleanflow Plus across the remaining tower cells, with continued monitoring of air-side pressure drop, specific fan power, and seasonal wet-bulb sensitivity. The CTI ATC-105–compliant field methods used in this study also provide a robust basis for cell-to-cell comparison and align with reliability-centered maintenance practices for heavy-duty industrial cooling equipment.

Declaration of AI and AI Assisted Technologies in the Writing Process

During the preparation of this work, the authors used Claude (Anthropic AI language model) in order to:

1) Refine the language and clarity of technical writing
2) Verify calculations and numerical accuracy of tables
3) Assist in organizing and structuring sections for better readability
4) Support in proofreading and ensuring consistency in terminology

After using this tool/service, the author reviewed and edited the content as needed and takes full responsibility for the content of the publication. The substantive scientific contributions, data interpretation, and conclusions are entirely the author's own work.

Declaration of Competiting Interest

The authors declare that they have no known competing financial interests or personal relationships that could have appeared to influence the work reported in this paper.

Acknowledgements

The author acknowledges Diponegoro University for academic support and John Cockerill Hamon for providing the opportunity to conduct this study using industrial cooling tower data during professional employment.

References

[1] Eurovent Middle East. (2021). Evaporative cooling and cooling towers: Guidebook (1st ed.). Retrieved from https://www.eurovent.eu/wp-content/uploads/2021-11-23-eme-ct-guidebook-first-edition-en-web-1.pdf

[2] Primo, J. (2020). Cooling towers: Basic calculations (Course M374). PDH Online. Retrieved from https://pdhonline.com/courses/m374/m374content.pdf

[3] Purdue University. (2024). Cooling tower heat and mass transfer processes (Lecture Notes SM-3). School of Mechanical Engineering. Retrieved from https://www.purdue.edu/freeform/me418/wp-content/uploads/sites/30/2024/09/Chapter-SM-3-Heat.pdf

[4] Hashemi, Z., Zamaniard, A., Gholampour, M., Liaw, J. S., & Wang, C. C. (2023). Recent progress in film media technology for wet cooling towers. Processes, 11(11), 2578. https://doi.org/10.3390/pr11092578

[5] Liao, J., et al. (2024). Optimization of corrugated sheet packing structure based on falling film flow characteristics. Applied Thermal Engineering, 229, 121563. https://doi.org/10.1016/j.applthermaleng.2024.121563

[6] Navarro, P., Ruiz, J. A., Kaiser, A., & Lucas, M. (2023). Effect of fill length and distribution system on the thermal performance of an inverted cooling tower. Applied Thermal Engineering, 231, 120876. https://doi.org/10.1016/j.applthermaleng.2023.120876
[7] SPX Cooling Technologies. (2024). Purposes and types of fills (CTII-02A). Retrieved from https://spxcooling.com/wp-content/uploads/CTII-02A.pdf
[8] SPX Cooling Technologies. (2024). Evaporative and water usage: Basic theory and practice. Retrieved from https://spxcooling.com/wp-content/uploads/AE-AS-24-1.pdf
[9] Shinde, S. S., et al. (2016). Analysis of the effect of packing materials (fills) and flow rate on the area and effectiveness of evaporative cooling tower. Energies, 14, 5255–5263. https://doi.org/10.3390/en16145355
[10] Cooling Technology Institute (CTI). (2000). ATC-105: Acceptance test code for water cooling towers.
[11] Wheeler, D. E., & Hennon, K. (2020). Review of new 2019 CTI ATC-105 acceptance test code for cooling towers. Clean Air Engineering.
[12] Araújo, D. S. O., et al. (2024). Comparative study of cooling tower fills: Experimental analysis and CFD simulation of an alternative fill. Brazilian Journal of Chemical Engineering, 46, 412–424. https://doi.org/10.1016/j.bjce.1007/4043-01024-04990-z
[13] Matjuba, M. M. (2025). Leveraging machine learning to optimize cooling tower efficiency for sustainable power generation. Frontiers in Energy Research, 13, 2025. https://doi.org/10.3389/fenrg.2025.1473946
[14] ASME. (2025). A dynamic model for performance and efficiency of evaporative cooling towers. ASME Journal Manuscript, 11, 4069. https://doi.org/10.1115/1.46070699
[15] Joshi, D. (2016). Cooling tower performance and determining energy saving opportunities through economizer operation: A review. IOSR Journal of Mechanical and Civil Engineering, 13(1), 1–12.
[16] Celenza, S., & Shank, O. (2019). Optimize water and energy use in evaporative cooling towers. Chemical Engineering Progress, June 22–25.
[17] Chen, H. C. (2025). Cooling towers: Balancing efficiency, water, and sustainability. Chemical Engineering Progress, May 22, 2025.
[18] Rohani, S., & Ahmadi, H. (2017). Retrofit of a wet cooling tower to reduce water and fan power consumption using a wet/dry approach. Applied Thermal Engineering, 2017.
[19] Safta, S. D., Kareem, A. M. G., & Chauf, A. (2023). Experimental and numerical analysis of the forced draft wet cooling. Journal of Thermal Engineering.
[20] Dmitriev, A. V., Zinovieva, O. S., & Madyshev, N. N. (2021). Experimental investigation of fill pack impact on thermal-hydraulic performance of evaporative cooling tower. Thermal Science and Engineering Progress.
[21] Okari, I., Sodiq, J. A., & Leo, F. (2025). Evaluation of cooling tower performance in a process plant.
[22] Al-Bloushi, M., Ahmed, Y., Al-Wazzan, N., Al-Mutairi, A., & Al-Rashidi, A. (2017). Effect of organic and chemical oxidation on biofouling control in pilot-scale seawater cooling towers. Journal of Water Process Engineering.
[23] Çengel, Y. A. (2003). Heat transfer: A practical approach (2nd ed.). McGraw-Hill.
[24] Qalbi, M. A., Suharto, B. H., & Wuryanti, Y. (2024). Analysis efektivitas cooling tower sebelum dan sesudah penggantian filler pack.
[25] Widodo, S. (2014). Improving analysis of risk-based maintenance management strategies through reliability centered maintenance: Case study coal crushing plant. Advance Sustainable Science, Engineering and Technology (ASSET), 6(2).
[26] Hamon. (2015). Hamon wet cooling systems. Hamon Group.
[27] Incropera, F. P., DeWitt, D. P., Bergman, T. L., & Lavine, A. S. (2007). Fundamentals of heat and mass transfer (6th ed.). Wiley.